



## Identification and molecular characterization of the high-affinity copper transporters family in *Solanum lycopersicum*

Paco Romero<sup>\*,1</sup>, Alessandro Gabrielli<sup>1</sup>, Raúl Sampedro<sup>1</sup>, Ana Perea-García<sup>2</sup>, Sergi Puig, María Teresa Lafuente

Department of Food Biotechnology, Institute of Agrochemistry and Food Technology (IATA-CSIC), Catedrático Agustín Escardino 7, 46980 Paterna, Valencia, Spain

### ARTICLE INFO

#### Keywords:

Heavy metal stress  
COPT  
Tomato

### ABSTRACT

Copper (Cu) plays a key role as cofactor in the plant proteins participating in essential cellular processes, such as electron transport and free radical scavenging. Despite high-affinity Cu transporters (COPTs) being key participants in Cu homeostasis maintenance, very little is known about COPTs in tomato (*Solanum lycopersicum*) even though it is the most consumed fruit worldwide and this crop is susceptible to suboptimal Cu conditions. In this study, a six-member family of COPT (SICOPT1-6) was identified and characterized. SICOPTs have a conserved architecture consisting of three transmembrane domains and  $\beta$ -strains. However, the presence of essential methionine residues, a methionine-enriched amino-terminal region, an Mx<sub>3</sub>Mx<sub>12</sub>Gx<sub>3</sub>G Cu-binding motif and a cysteine rich carboxy-terminal region, all required for their functionality, is more variable among members. Accordingly, functional complementation assays in yeast indicate that SICOPT1 and SICOPT2 are able to transport Cu inside the cell, while SICOPT3 and SICOPT5 are only partially functional. In addition, protein interaction network analyses reveal the connection between SICOPTs and Cu P<sub>1B</sub>-type ATPases, other metal transporters, and proteins related to the peroxisome. Gene expression analyses uncover organ-dependency, fruit vasculature tissue specialization and ripening-dependent gene expression profiles, as well as different response to Cu deficiency or toxicity in an organ-dependent manner.

### 1. Introduction

Copper (Cu) is a micronutrient that plays a dual role for living beings as it is an essential redox cofactor, but it is toxic when in excess. Sub-optimal Cu levels in human diet can cause impaired neurological development and cardiovascular problems, Menkes/Wilson and Addison metabolic disorders and Alzheimer's disease [1–6]. In plants, Cu plays important roles in key processes, namely photosynthesis, respiration, superoxide scavenging and hormone perception [7,8]. Low Cu levels may result in impaired pollen development and viability, responses to iron deficiency and reduced disease resistance, but its toxicity causes DNA damage, chlorosis and root growth inhibition, among other

symptoms [7,9–16]. As plants constitute the main entrances of micronutrients in trophic chains, and their nutritional deficiencies or excesses are often transferred to consumers [7], understanding Cu uptake and distribution to edible plant parts is crucial for coping with deficient or toxic Cu levels that may ultimately affect human health.

To deal with Cu's dual nature, plants have a sophisticated homeostasis network whereby Cu uptake is tightly, but dynamically, regulated. The equilibrium between Cu-demanding and Cu-toxicity is balanced under Cu stress conditions [17–19]. Most plants can obtain free Cu<sup>2+</sup> from soil through promiscuous divalent transporters (YSL, ZIP) [15,20,21]. When Cu<sup>2+</sup> bioavailability is reduced as a result of soil alkalization or high organic matter content, among others, the root

**Abbreviations:** ABA, Abscisic acid; BCS, Bathocuproinedisulfonic acid disodium; BPS, Bathophenanthrolinedisulfonic acid; COPT, Copper transporters; GGR, Green germination rate; ROS, Reactive oxygen species; SC, Synthetic complete medium; SOD, Superoxide dismutase; TMD, Transmembrane domain; YPD, Yeast extract/peptone/dextrose; YPEG, Yeast extract/peptone/ethanol/glycerol.

\* Corresponding author.

**E-mail addresses:** [promero@iata.csic.es](mailto:promero@iata.csic.es) (P. Romero), [agagar4@alumni.uv.es](mailto:agagar4@alumni.uv.es) (A. Gabrielli), [rsampedro@iata.csic.es](mailto:rsampedro@iata.csic.es) (R. Sampedro), [ana.perea@uv.es](mailto:ana.perea@uv.es) (A. Perea-García), [spuig@iata.csic.es](mailto:spuig@iata.csic.es) (S. Puig), [mtlafuente@iata.csic.es](mailto:mtlafuente@iata.csic.es) (M.T. Lafuente).

<sup>1</sup> Both authors contributed equally to conduct this work and must be considered *first authors*.

<sup>2</sup> Current address: Departament de Bioquímica i Biologia Molecular and Estructura de Recerca Interdisciplinària en Biotecnologia i Biomedicina (ERI BIOTECMED), Universitat de València, C/ Dr. Moliner, 50, 46100 Burjassot, Valencia, Spain

<https://doi.org/10.1016/j.ijbiomac.2021.10.032>

Received 17 June 2021; Received in revised form 27 September 2021; Accepted 3 October 2021

Available online 13 October 2021

0141-8130/© 2021 The Authors. Published by Elsevier B.V. This is an open access article under the CC BY license (<http://creativecommons.org/licenses/by/4.0/>).

surface is acidified through H<sup>+</sup> ATPases, and Cu<sup>2+</sup> is reduced to soluble Cu<sup>+</sup> using plasma membrane ferric reductase oxidases [1,22,23]. Then Cu<sup>+</sup> is collected and transported through the plasma membrane using the CTR/COPT members of the high-affinity copper transporter family, which are considered the main contributors to initial Cu uptake in plants [10,24–26].

The alignment of COPT family members from different species [27] reveals a highly conserved structure model that contains three putative transmembrane domains (TMD1–3). At sequence level, a methionine (M)-enriched amino-terminal (N-terminal) region and a carboxy-terminal (C-terminal) region rich in cysteine (C) residues are also present in most of the COPT members described. In *Arabidopsis*, the M-rich motif sequesters Cu<sup>+</sup> from the extracellular matrix to translocate it to the cytosol. For that function, an M residue 20 amino acids before TMD1 and an Mx<sub>3</sub>M motif within TMD2 are essential. A Gx<sub>3</sub>G motif within TMD3 is fundamental for the packing and assembly of CTR/COPTs, which can homotrimerize or build heterocomplexes with other COPT members or other proteins to form a pore in the membrane [28,29]. It is noteworthy that the simultaneous presence of the Mx<sub>3</sub>Mx<sub>12</sub>Gx<sub>3</sub>G signature is reported to be strictly conserved in all functional CTR/COPT members [30]. Last, the CxC motif in the C-terminal region participates in sensing high intracellular Cu levels and in transferring Cu to cytosolic metal-chaperones [31], which distribute Cu to different organelles where cuproproteins like plastocyanin, cytochrome *c* oxidase (COX) or the ethylene receptor require this element to function [22]. Another regulation step of this dynamic network relies on the transcriptional activation of Cu deficiency-responsive genes by the SQUAMOSA promoter binding protein-like 7 (SPL7) transcription factor, which binds to *cis*-regulatory GTAC motifs in the promoter region of these genes [32,33].

The COPT family has been identified in a number of crops, including alfalfa, maize, vine and rice [28,34–36]. However, no information is available on COPTs' function in tomato (*Solanum lycopersicum*), despite its undeniable importance for human diet as the most consumed fruit worldwide. Despite mentioning three putative Cu transporters for *S. lycopersicum* [27], detailed information on their functionality, interaction networks or transcriptional regulation remains unknown. So there are no reports characterizing the proteins responsible for Cu uptake in tomato plants despite the documented detrimental effects of Cu deficiency on plant physiology and yields [37–40]. In this work, six tomato COPT family members were genome-wide identified and characterized with a set of *in silico* analyses. Their functionality was studied by yeast heterologous expression complementation, and the tissue-dependent effects of Cu availability on gene expression profiles were analyzed by *in vitro* assays. This is the first approach to understand the molecular mechanisms underlying Cu homeostasis in tomato and how COPT transporters might help to develop agricultural strategies that cope with inadequate micronutrient bioavailability.

## 2. Materials and methods

### 2.1. Identification of the COPT transporter family members in *Solanum lycopersicum*

In order to identify the putative COPT genes in *Solanum lycopersicum* (SICOPTs), the protein sequences of the *Arabidopsis thaliana* COPTs (AtCOPT1–AtCOPT6) were retrieved from the UniProtKB/SwissProt database of NCBI ([ncbi.nlm.nih.gov](http://ncbi.nlm.nih.gov)) and used as queries in the BLASTP program against the tomato genome in the Phytozome database ([phytozome.jgi.doe.gov/pz/portal](http://phytozome.jgi.doe.gov/pz/portal)) with an e-value threshold of -10. Redundant sequences were removed and six putative Cu transporter sequences of *Solanum lycopersicum* were left for this study. Genome and CDS sequences were obtained from this database and used in the Gene Structure Display 2.0 [41] to obtain the number and organization of the exons/introns of SICOPTs. The PSIPRED server [42] was used to determine protein sequence length, to calculate both molecular weight (Mw) and the theoretical isoelectric point (pI), and to predict the subcellular

location. The sequence of the promoter regions (1.5 Kb upstream of 5'-UTR) of the SICOPT genes were also obtained from the Phytozome database and their *cis*-acting elements were identified by the New PLACE program [43].

### 2.2. Sequence conservation and phylogenetic analyses

The multiple sequence alignments of the *S. lycopersicum* and *A. thaliana* COPTs were performed with the Clustal Omega program [44] and represented using DNAMAN ([lynonn.com/dnaman](http://lynonn.com/dnaman)). The grape (*Vitis vinifera*), maize (*Zea mays*), rice (*Oryza sativa*), poplar (*Populus trichocarpa*), lotus (*Lotus japonicus*), field mustard (*Brassica rapa*), wild cabbage (*Brassica oleracea*), stiff brome (*Brachypodium distachyon*) and yeast (*Saccharomyces cerevisiae*) species were also selected as representative organisms to study phylogenetic COPTs similarities with tomato (*Solanum lycopersicum*). The COPT sequences for these species were also retrieved from the Phytozome database. Based on these alignments, phylogenetic trees were constructed by a Neighbor-Joining algorithm with 1000 bootstrap replications, without distance corrections and according to the Newick format. The circular phylogenetic trees were visualized with the interactive Tree of Life software [45]. The conservation of the Cu binding domain in SICOPTs was evaluated by the WebLogo3 software [46] using the 22-residues of the Mx<sub>3</sub>Mx<sub>12</sub>Gx<sub>3</sub>G sequence.

### 2.3. Protein modeling and interaction network analysis

The prediction of both the transmembrane spanning domains and secondary protein structures was performed with the PSIPRED server [42] and schematically represented with CorelDraw (Graphics Suite). The tertiary structures of SICOPTs were predicted by the I-TASSER server [47], in which the crystallographic structure of the homotrimeric Ctr1 transporter from *Salmo salar* was used as a template [48]. The protein network structures of SICOPTs were predicted based on their amino acid sequences by the STRING 10.0 server [49], which harbors putative interactions from curated databases. These interactions include direct (physical) and indirect (functional) associations not only in plants but also in other kingdoms. These interactions stem from computational prediction, from knowledge transfer between organisms, and from interactions aggregated from other (primary) databases, all derived from sources including genomic context predictions, high-throughput experiments, (conserved) co-expression and automated textmining. The default settings of 10 first-shell interactors were used, and up to five interactions in the second shell were added.

### 2.4. Plasmid constructs and functional complementation experiments in yeast

The coding sequences of the five SICOPT family members showing a theoretically functional Cu binding domain (SICOPT1, SICOPT2, SICOPT3, SICOPT5, SICOPT6) were amplified from the cDNA samples using the specific primers detailed in Table S1, and were subcloned into the BamHI/EcoRI restriction enzyme site of yeast multicopy expression vector p426GPD [50], which generated five different plasmids (p426GPD/SICOPTs). A p426GPD/AtCOPT1 plasmid, containing the coding sequence of *A. thaliana* COPT1, was provided by Dr. Peñarrubia's Lab (UV, Valencia, Spain). All the plasmids constructed in this study were sequenced at the Genome Facility at the Servei Central de Suport a la Investigació Experimental (SCSIE-UV, Valencia, Spain). Thereafter, the MPY17 (MATa, *ctr1::ura3::KanR*, *ctr3::TRP1*, *his3*, *lys2-802*, *CUIP1R*) strain was transformed with p426GPD (negative control), p426GPD/AtCOPT1 (positive control) or one of the five p426GPD/SICOPTs, and grown in synthetic complete medium without uracil (SC-Ura) to OD<sub>600</sub> = 0.1 as described in [51]. To perform the complementation assay, two 10-fold serial dilutions were plated on SC-Ura, SC-Ura supplemented with ferrozine (300 μM), SC-Ura supplemented with

bathophenanthrolinedisulfonic acid (BPS, 50  $\mu\text{M}$ ), YPD (2% glucose), YPEG (2% ethanol, 3% glycerol) or YPEG supplemented with Cu (100  $\mu\text{M}$   $\text{CuSO}_4$ ). Plates were incubated for 3 (SC-Ura, YPD, YPEG, YPEG+Cu) or 7 (SC-Ura + Ferrozine, SC-Ura + BPS) days at 30 °C and photographed with a Nikon Z5 camera (Nikon Corporation).

### 2.5. *In silico* analysis of gene expression

The expression data of the *SICOPT* genes in the different organs and several fruit tissues during ripening were retrieved from TomExpress database [52] and the Tomato Expression Atlas database [53–55], respectively.

### 2.6. Plant growth and treatments

Tomato (*S. lycopersicum* L. cv. Moneymaker) seeds were surface-sterilized with sequential washes in 50% bleach (5 min) and water ( $2 \times 15$  min), and stratified for 2 days at 4 °C. Then they were sown on plates containing home-made  $\frac{1}{2}$  MS medium [56] supplemented with 1% sucrose (*w/v*) and 0.8% agar at pH 5.6. To generate Cu deficiency (Cu 0  $\mu\text{M}$ ), the components of  $\frac{1}{2}$  MS medium [56] were prepared separately according to the following conditions: macronutrients (10.3 mM  $\text{NH}_4\text{NO}_3$ , 9.4 mM  $\text{KNO}_3$ , 0.37 mM  $\text{MgSO}_4$ , 0.62 mM  $\text{KH}_2\text{PO}_4$  and 1.13 mM  $\text{CaCl}_2$ ), micronutrients (50.1  $\mu\text{M}$   $\text{H}_3\text{BO}_3$ , 50  $\mu\text{M}$   $\text{MnSO}_4$ , 15  $\mu\text{M}$   $\text{ZnSO}_4$ , 0.52  $\mu\text{M}$   $\text{NaMoO}_4$  and 0.05  $\mu\text{M}$   $\text{CoCl}_2$ ), 50  $\mu\text{M}$  Fe-EDTA, 2.5  $\mu\text{M}$  KI and 0.05% MES. To generate Cu sufficiency and excess conditions, increasing  $\text{CuSO}_4$  concentrations were added to  $\frac{1}{2}$  MS medium. For severe Cu-deficient conditions,  $\frac{1}{2}$  MS was supplemented with increasing amounts of Cu chelator bathocuproinedisulfonic acid disodium (BCS). Seeds were germinated in capped sterile cups under the selected Cu bioavailability range conditions and grown in a neutral day photoperiod (12 h light, 23 °C/12 h darkness, 16 °C) in a Sanyo Growth Cabinet MLR-350 T (65 mmol  $\text{m}^{-2}$  cool-white fluorescent light) for 21 days. All the conditions were composed of three independent cups (replicates), each containing five seeds. The green germination rate (GGR) was calculated as the percentage of germinated seeds that developed true leaves to the total sown seeds.

### 2.7. RNA isolation and gene expression by real-time qPCR

Total RNA was extracted separately from the roots, stems and leaves of the 21-day-old seedlings grown under the conditions indicated in Section 2.6. For root and stem tissues, RNA was extracted by the RNAeasy mini plant kit (Qiagen) following the manufacturer's instructions, while leaf tissue RNA was extracted with Trizol reagent as described in [57]. RNA was quantified spectrophotometrically and its integrity was assessed by agarose gel staining. cDNA was synthesized as in [58], and real-time quantitative PCRs were carried out with SYBR Green qPCR MasterMix (Roche) by using specific primers (Table S1) as described in [59]. Relative expression assays were analyzed by the Relative Expression Software Tool (REST, [rest.gene-quantification.info](http://rest.gene-quantification.info)).

### 2.8. Statistical analyses

A one-way ANOVA test and Tukey's *post hoc* test were applied to determine the significance of the mean GGR and relative gene expression values at  $P \leq 0.05$  by the Statgraphics Plus 4.0 software (Manugistics, Inc.). All the data represent the mean value of three biological replicates  $\pm$  standard error.

## 3. Results

### 3.1. The COPT family in *Solanum lycopersicum*

Six *Solanum lycopersicum* COPT genes encoding putative CTR/COPT transporters were found in the tomato genome, and designated as

*COPT1* through to *COPT6* (alias *SICOPT1-SICOPT6*) (Table 1). The encoded proteins had a similarity to the *Arabidopsis* COPTs that ranged from 37% (*SICOPT4*) to 77% (*SICOPT5*). The most similar proteins to *SICOPTs* were found in the *Solanum tuberosum* genome, with similarities above 94% for all cases, except for *SICOPT2* (71%) and *SICOPT4* (59%) (Table 1). Every *SICOPT* was located in a different chromosome, except for *SICOPT3* and *SICOPT6* that were located in chromosome IX, which suggests that these members are paralogues (Table 2). The length of their coding sequences (CDS) ranged from 402 bp (*SICOPT3*) to 519 bp (*SICOPT2*), with the corresponding encoded proteins ranging from 133 to 172 residues, respectively. The molecular weights of *SICOPTs* varied from 15.29 kDa (*SICOPT3*) to 18.77 kDa (*SICOPT2*), and the theoretical isoelectric points showed basic protein nature and ranged from 7.6 (*SICOPT6*) to 10.1 (*SICOPT4*) (Table 2). All the *SICOPTs* were predicted to have three transmembrane domains (TMD) and to be most probably located at the plasma membrane. Moreover, *SICOPT3* and *SICOPT4* were predicted to be associated with lysosome and cytosol to some extent, respectively. Of *SICOPTs*, only *SICOPT2* and *SICOPT4* had introns in their genome sequences. *SICOPT2* had one intron of about 200 bp long, while *SICOPT4* had two introns of about 50 and 1300 bp long (Table 2 and Fig. S1).

### 3.2. Sequence alignment and phylogenetic analyses

Protein sequence alignment was performed with the six *SICOPTs* and the *A. thaliana* COPT1 as a conserved model of the COPT family in plants (Fig. 1A). The results showed that the most noticeable divergences among *SICOPT* members were localized around the N-terminal and C-terminal regions. Through the COPT sequences, two different regions showed a high number of conserved residues. The sequences located between these two regions were vastly variable. The Cu binding domain sequence (Mx<sub>3</sub>Mx<sub>12</sub>Gx<sub>3</sub>G) and an M residue located 20 residues before TMD1 on the N-terminal extreme were highly conserved among all the *SICOPTs*, except *SICOPT4* (Fig. 1). The CxC motif at C-terminal was found only in *SICOPT1*, *SICOPT2* and *SICOPT5* (Fig. 1A). A phylogenetic analysis revealed that *SICOPTs* were divided into three main branches when were analyzed together with the *AtCOPT* members (Fig. 1D). *SICOPT5* clustered together with its *Arabidopsis* ortholog on a separate branch. Another clade was composed of two subgroups, the first contained *SICOPT4* and its ortholog *AtCOPT4*, and the second was formed only by tomato COPT members (*SICOPT1*, *SICOPT2* and *SICOPT3*). Last, other *Arabidopsis* COPTs (*AtCOPT2*, *AtCOPT6*, *AtCOPT1* and *AtCOPT3*) clustered together, and *SICOPT6* was their closest tomato ortholog (Fig. 1D). These results agree with the similarity matrix among these species' COPT members (Table S2). In order to find similarities to other plant species, the COPT members of *V. vinifera*, *Z. mays*, *O. sativa*, *B. rapa*, *B. oleracea*, *P. trichocarpa*, *L. japonicus*, *B. distachion* and *S. cerevisiae* were included in the phylogenetic analysis (Fig. S2). Overall, the analysis revealed that *SICOPTs* were closer to those from *V. vinifera* than to *Arabidopsis* or the monocots species. These results were consistent with the previous phylogenetic analyses that clustered together *SICOPT4* and *AtCOPT4*, and separated them from the rest of their respective family members (Fig. 1D). *SICOPT5* and *AtCOPT5* also remained close and grouped on the same branch with other vine members (*VvCOPT1*, *VvCOPT7* and *VvCOPT8*). *SICOPT3* separated from the other members of its family to cluster with *VvCOPT5* and *VvCOPT6*. In this analysis, *SICOPT6* grouped closer to *SICOPT1* and *SICOPT2* than to the *AtCOPTs*, but was still closer to *VvCOPT2* and *VvCOPT4* than to its family members in *S. lycopersicum* (Fig. S2).

### 3.3. Protein structure and interaction networks of the *SICOPT* family

The secondary structures of the *SICOPTs* were composed of an M-rich region on the N-terminal extreme, followed by two  $\beta$ -strands, three TMDs (TMD1-3) and a last  $\beta$ -strand near the Ct region (Fig. 2). The number of predicted  $\beta$ -strands and TMD was constant in *SICOPTs*. All the

**Table 1**  
Identification of the COPT transporters in the *S. lycopersicum* genome.

Gene ID (Phytozome)	NCBI protein accession	Short name	Comparison with <i>Arabidopsis</i>		Most similar	
			Gen - Description	Similarity	Homolog / Similarity	Organism. Description
<i>Solyc08g006250</i>	XP_004244480.1	SICOPT1	AT3G46900.1 - copper transporter 2	68.4%	PGSC0003DMT400024665 / 96.8%	<i>Solanum tuberosum</i> . Copper transporter
<i>Solyc06g005820</i>	XP_004240384.1	SICOPT2	AT5G59030.1 - copper transporter 1	71.3%	PGSC0003DMT400053688 / 71.5%	<i>S. tuberosum</i> . Copper transporter
<i>Solyc09g011700</i>	XP_004246857.3	SICOPT3	AT3G46900.1 - copper transporter 2	59.4%	PGSC0003DMT400030604 / 94.7%	<i>S. tuberosum</i> . Copper transporter
<i>Solyc10g084980</i>	XP_004252993.1	SICOPT4	AT2G37925.1 - copper transporter 4	37.2%	PGSC0003DMT400028798 / 58.8%	<i>S. tuberosum</i> . Copper transporter
<i>Solyc02g082080</i>	XP_004232609.1	SICOPT5	AT5G20650.1 - copper transporter 5	77.2%	PGSC0003DMT400035520 / 98.7%	<i>S. tuberosum</i> . Copper transporter
<i>Solyc09g014870</i>	XP_019071080.1	SICOPT6	AT2G26975.1 - copper transporter 6	66.0%	PGSC0003DMT400059564 / 97.9%	<i>S. tuberosum</i> . Copper transporter

**Table 2**  
Characterization of the COPT transporters identified in *S. lycopersicum*.

Short name	Chromosome location	CDS length (bp)	Protein length (aa)	Mw (kDa)	Intron number	pI	TM domains	Predicted intracellular location (probability)
<i>SICOPT1</i>	VIII	468	155	16.29	0	8.3	3	PM (0.95)
<i>SICOPT2</i>	VI	519	172	18.77	1	8.1	3	PM (1.00)
<i>SICOPT3</i>	IX	402	133	15.29	0	7.7	3	PM (0.66); Ly (0.22)
<i>SICOPT4</i>	X	447	148	17.09	2	10.1	3	PM (0.66); Cy (0.16)
<i>SICOPT5</i>	II	450	149	16.84	0	8.8	3	PM (0.94)
<i>SICOPT6</i>	IX	426	141	15.66	0	7.6	3	PM (0.94)

members save SICOPT4 displayed a separation of 2-4 residues between TMD2 and TMD3 which, in turn, contained the Mx<sub>3</sub>Mx<sub>12</sub>Gx<sub>3</sub>G sequence (Cu binding domain). In SICOPT4, TMD2 and TMD3 were more distant, the Cu binding domain was not conserved, and no M-rich region on the N-terminal extreme was found (Fig. 2A). Tertiary structure modeling was achieved by using the Ctr1 of *Salmo salar* as a template (Fig. 2B). SICOPTs' structures mostly overlapped the template's tertiary structure in relation to the  $\alpha$ -helices and  $\beta$ -strands. It was noteworthy that SICOPT2, SICOPT4 and SICOPT5 showed extended  $\alpha$ -helix structures according to the lengths in the model, but the overlapping in the remaining sequence was as good as it was for other family members.

In order to investigate the relations among SICOPTs and with the other proteins encoded in the tomato genome, a protein interaction networks analysis was performed (Fig. 2C and Fig. S3). As with the interaction among SICOPTs members, only SICOPT4 and SICOPT5 showed a direct relation. The analysis of the interaction of SICOPTs with other proteins revealed a general pattern in which several specificities were found depending on the SICOPT member. In general, SICOPTs associated with a number of metal transporter proteins, including those related to iron (OPT), magnesium (MRS) and zinc (ZIP and ZRT/IRT-like). They also interacted with several proteins involved in Cu homeostasis, such as cupro-chaperones (CCH, CCS, COX11 and ATOX1), Cu ATPases (RAN1, HMAs, PAA1 and ATP7), and the transcription factor SPL7. In addition, all the SICOPTs interacted with a protein phosphatase type 2C (PP2C) that, in turn, related to protein kinases (YAK1 and DYRKP-3) and a set of proteins associated with the peroxisome (PEX7, PEX5 and PEX10). It is worth noting that SICOPT3 and SICOPT5 did not interact with SPL7, SICOPT4 did not relate to other metal transporters, and SICOPT5 interacted with zinc (Zn) rather than with iron (Fe) and magnesium (Mg) transporters as observed in the other family members (Fig. 2C and Fig. S3).

### 3.4. Functional complementation in the *S. cerevisiae* *ctr1Δctr3Δ* mutant

In order to confirm the Cu transporter function of SICOPTs, growth assays were independently carried out for those SICOPT members showing a theoretically functional Cu binding domain in a *S. cerevisiae* *ctr1Δctr3Δ* mutant defective for Cu transport through the plasma

membrane (Fig. 3). All the strains were able to grow on control SC-Ura and YPD media. On YPEG medium, which contains ethanol and glycerol as the only carbon sources and renders using Cu for respiratory growth necessary, the *ctr1Δctr3Δ* cells carrying the empty vector could not survive, but normal growth was restored by the expression of SICOPT1 and SICOPT2. The vectors containing the CDS of SICOPT3 and SICOPT5 showed slightly recovered growth in this medium. In contrast, the expression of SICOPT6 did not rescue the defective growth of the *ctr1Δctr3Δ* mutant in YPEG. As expected, all the above-described strains grew in YPEG medium when supplemented with Cu. To further test the functionality of SICOPTs, transformed yeast cells were grown on Fe-deficient media achieved by adding Fe<sup>2+</sup>-specific chelators Ferrozine or BPS. Yeast cell growth under low Fe conditions requires Cu because it is an essential cofactor for the Fet3-Ftr1 high-affinity Fe uptake system. The expression of SICOPT1 and SICOPT2 allowed cells to grow under these conditions, while a slight partial growth recovery was observed with the expression of SICOPT3 and SICOPT5, mostly under the Fe-deficient conditions caused by Ferrozine. SICOPT6 expression did not rescue the defective Cu uptake in the *ctr1Δctr3Δ* mutant in the absence of Fe (Fig. 3). The complete growth recovery of a yeast mutant defective in Cu uptake under both respiratory and iron-deficient conditions by SICOPT1 and SICOPT2 strongly suggested that both proteins functioned as cell surface Cu transporters.

### 3.5. Identification of cis-elements in the SICOPTs promoter region and in silico gene expression analyses

The sequences of the 1.5 Kb upstream region of the translation start site of the SICOPTs genes were analyzed to investigate the presence of putative cis-elements (Table 3). Several Cu responsive elements (CuRE, GTAC motif) were found, with a notably larger number in SICOPT2, SICOPT5 and SICOPT6 (16) than in SICOPT4 (8), SICOPT3 (4) or SICOPT1 (2). In contrast, only SICOPT1 showed one IRO2 element related to Fe deficiency. As regards the elements of response to macro-nutrients, the most abundant were those related to potassium, which were present in all the SICOPTs. Those related to sulfur were not found in SICOPT4, and only SICOPT5 presented two phosphate responsive elements. SICOPTs presented a large number of cis-elements related to

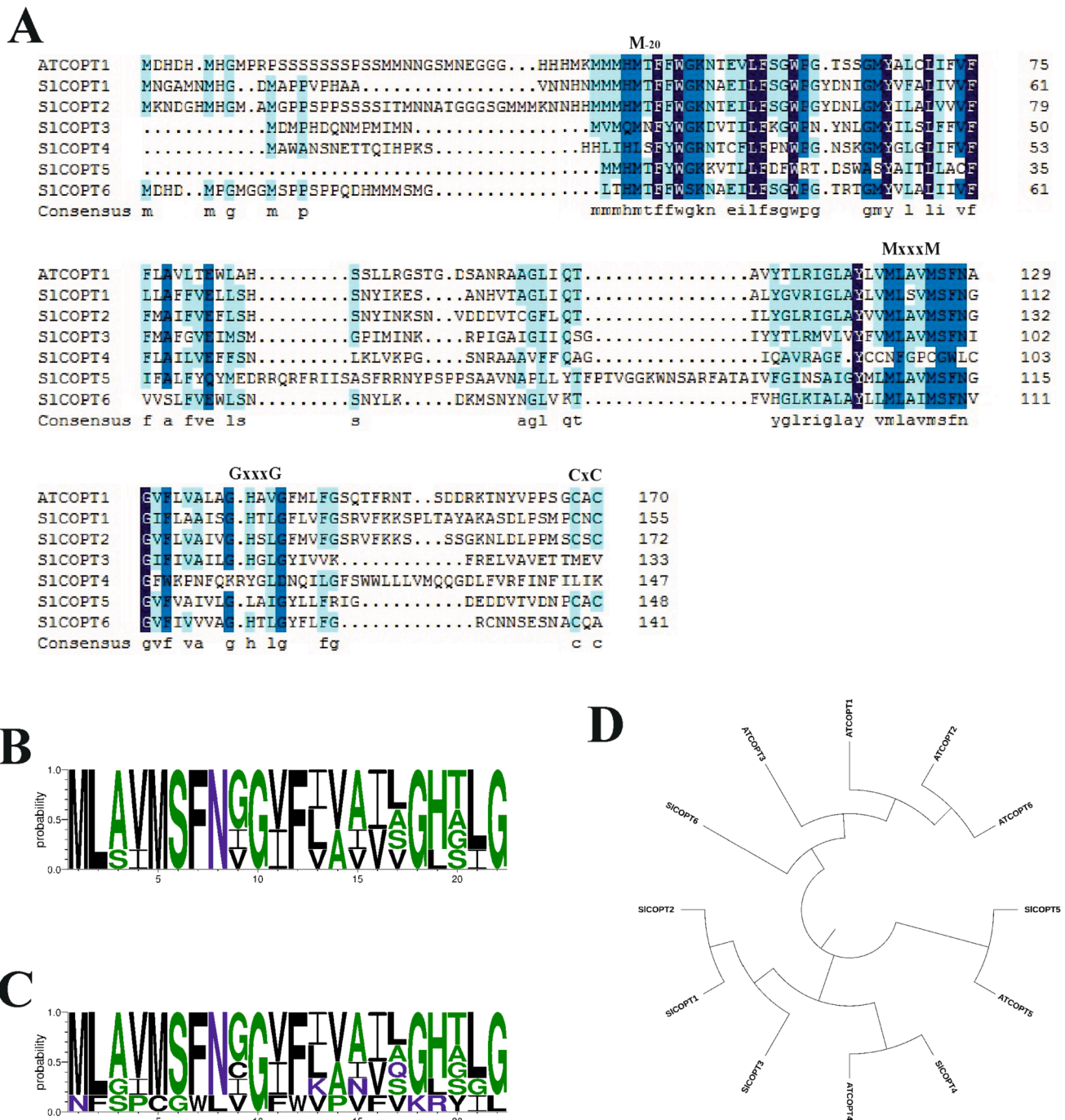


**Fig. 1.** Sequence conservation in SICOPTs. (A) Multiple alignment of the amino acid sequences of all the *S. lycopersicum* COPTs identified in this study and the *A. thaliana* COPT1. Identical residues are in black, highly conservative are depicted in dark blue and less conserved ones in light blue. The methionine 20 residues before TMD1 are indicated, as well as the Mx<sub>3</sub>M, Gx<sub>3</sub>G and CxC motifs. (B) Sequence logo representing the conserved residues in the 22 amino acids sequence of the Mx<sub>3</sub>Mx<sub>12</sub>Gx<sub>3</sub>G signature when considering all the SICOPTs or (C) excluding S1COPT4. (D) Phylogenetic analyses of the COPT family genes from *S. lycopersicum* and *A. thaliana*. Circular trees were constructed using neighbor-joining methods and 1000 bootstrap, and are represented with the iTol software. (For interpretation of the references to colour in this figure legend, the reader is referred to the web version of this article.)

organ- or tissue-specific gene expression. The most abundant were those related to seed, specifically endosperm tissue, followed by those related to the mesophyll and root. A number of motifs related to pollen-specific gene expression were also found in all the SICOPTs, while only S1COPT2 and S1COPT5 presented elements related to fruit-specific transcript regulation. Furthermore, all the SICOPTs contained different types of cis-elements related to hormone response, in which those related to abscisic acid (ABA) predominated. The responsive elements associated with ABA, cytokinins, gibberellic acid and auxins were found in all the

SICOPT members. The elements responsive to salicylic acid, ethylene and jasmonic acid were less abundant, and were not present in all the studied genes. Some biotic and abiotic stress-responsive cis-elements were also identified. Among those responsive to abiotic stresses, several types of light and water stress cis-elements were the most abundant and appeared in all the SICOPTs. In addition, responsive elements to wounding, temperature, O<sub>2</sub>/CO<sub>2</sub> and osmotic stresses were found. Among the response to biotic stresses, pathogen responsive elements were the most abundant. They were found in all SICOPTs, as well as the

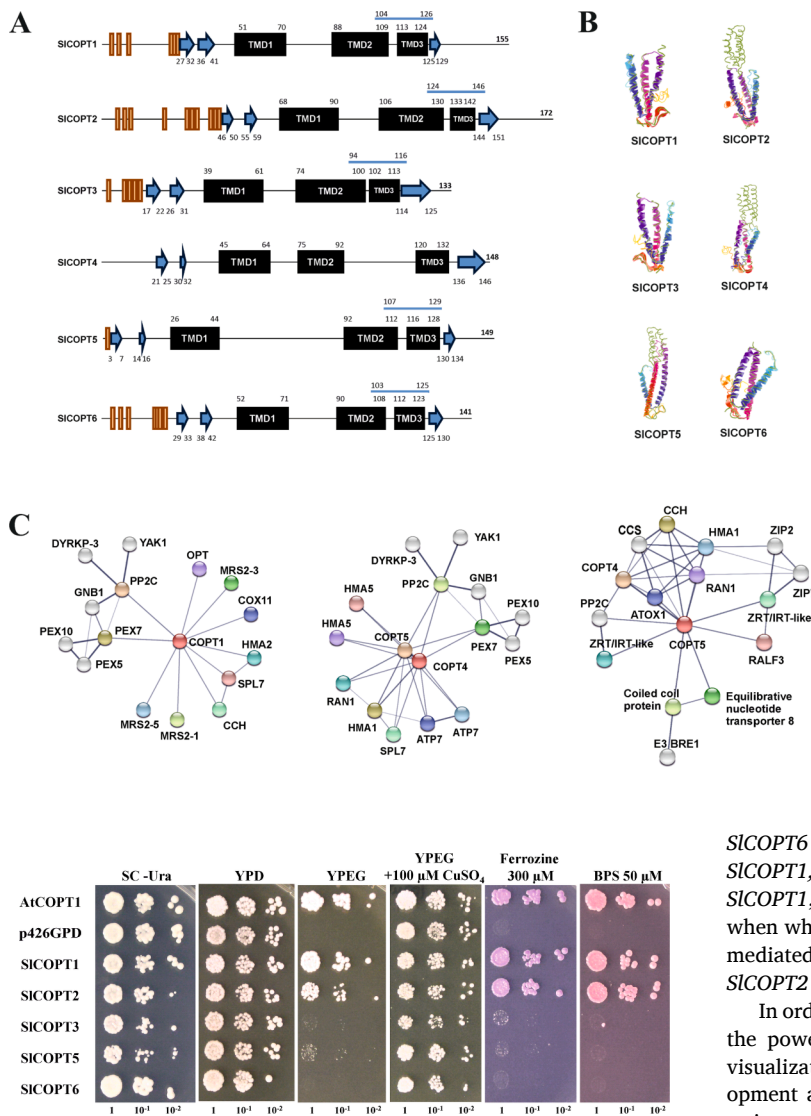


**Fig. 3.** Functional complementation of the *S. cerevisiae ctr1Δctr3Δ* mutant by the expression of the tomato *SICOPT1*, *SICOPT2*, *SICOPT3*, *SICOPT5* and *SICOPT6* genes. Yeast *ctr1Δctr3Δ* cells transformed with empty vector (p426GPD, negative control), *Arabidopsis thaliana* COPT1 (p426GPD-AtCOPT1, positive control) and SICOPT1-6 (p426GPD-SICOPT1-6) were assayed for Cu transport in different media. Two 10-fold serial dilutions of each transformant were grown for 3 (SC-Ura, YPD, YPEG, YPEG+Cu) or 7 (SC-Ura + Ferrozine, SC-Ura + BPS) days at 30 °C.

motifs related to disease resistance. The *cis*-elements related to the defense response were, however, identified only in the promoter sequence of *SICOPT1*, *SICOPT2* and *SICOPT6*. The presence of responsive elements associated with nodulation was also observed in all the *SICOPT* members. The regulation of *SICOPTs* gene expression by the circadian clock seemed limited to members *SICOPT1*, *SICOPT2*, *SICOPT3* and *SICOPT5*.

The gene expression data in the TomExpress database [52] allowed to study the transcriptional pattern of *SICOPTs* in different organs during plant development and in response to light/dark (sun/shade) stimuli. As shown in Fig. 4A, *SICOPT6* and *SICOPT3* were specifically expressed in roots, while *SICOPT2* was highly induced in flowers. *SICOPT1*, *SICOPT4* and *SICOPT5* were, however, specifically repressed in those organs and slightly induced in meristem and leaves during development. It is noteworthy that these three genes clustered together according to these expression patterns, while *SICOPT4* and *SICOPT5* grouped on a closer branch. In response to light (sun/shade experiments), *SICOPTs* were barely regulated in flowers, leaves and meristem (Fig. 4A). *SICOPT3* and

**Fig. 2.** Protein structure and interaction networks of *SICOPTs*. (A) Schematic representation of the secondary structure of *SICOPTs* predicted by PSIPRED. Orange boxes indicate methionine residues, blue arrows represent  $\beta$ -strands, and transmembrane domains (TMD) are depicted as black boxes. The Cu binding domain (Mx<sub>3</sub>Mx<sub>12</sub>Gx<sub>3</sub>G) is indicated by a blue line over the structure. Numbers denote the amino acid residue of the start and end of the corresponding secondary structure. *SICOPTs* are sorted by phylogenetic proximity. (B) Tertiary structure modeling according to I-Tasser and considering Ctr1 from *Salmo salar* to be a template. (C) The protein interaction networks of *SICOPT1*, *SICOPT4* and *SICOPT5*. Each node represents all the proteins produced by a single protein-coding gene locus. The colored and white nodes indicate the first (up to 10) and second (up to 5) shell of interactors, respectively. The name of each node was assigned according to the best hit match provided by STRING BLAST for each *S. lycopersicum* ID. (For interpretation of the references to colour in this figure legend, the reader is referred to the web version of this article.)

*SICOPT6* were highly induced by light in roots, as were *SICOPT5* and *SICOPT1*, but to a lesser extent. In stem, light induced the expression of *SICOPT1*, *SICOPT2* and *SICOPT5*, but repressed that of *SICOPT4*. Last, when whole seedling tissue was analyzed, *SICOPT1* and *SICOPT4* light-mediated inductions were observed, while this stimulus repressed *SICOPT2* expression.

In order to study the *SICOPTs* transcript levels in tomato fruit, we put the powerful TEA database [53–55] to good use, which allows the visualization of changes in gene expression during tomato fruit development and ripening at the tissue level (Fig. 4B). The *SICOPT6* transcripts were barely detected in any fruit tissue or development/ripening stage. For the other *SICOPT* members, two different expression patterns were deduced. The first was associated with the specialized expression of *SICOPT3*, *SICOPT4* and *SICOPT5* in vascular tissue, with a minimal relation to fruit ripening. Second, *SICOPT1* and *SICOPT2* showed opposite expression patterns associated with fruit development and ripening. It is worth mentioning that *SICOPT2* expression levels slightly varied with fruit development and ripening in seeds, and notably greater transcript accumulation was found in columella tissue in later stages.

### 3.6. Effects of Cu availability on *SICOPT* gene expression

There is no information in public tomato databases that allow the investigation of the regulation of *SICOPTs* under the stress caused by Cu deficiency or excess during growth. In this work, *in vitro* assays were designed to test the effect of a range of Cu availabilities on *SICOPTs* gene expression in the root, stem and leaf tissues of the 21-day-old seedlings. The GGR increased from BCS 100  $\mu$ M to reach a maximum at CuSO<sub>4</sub> 5  $\mu$ M (Fig. 5). Thereafter, the GGR lowered with CuSO<sub>4</sub> addition to growing media. Indeed, the GGR significantly dropped when seeds were sown at CuSO<sub>4</sub> 10  $\mu$ M, and bottomed down when this concentration was increased to CuSO<sub>4</sub> 100  $\mu$ M. The vigor of seedlings and root/stem development evolved according to the GGR (Fig. 5). Together, these results indicate for this tomato cultivar that: BCS 100  $\mu$ M and 50  $\mu$ M provoked severe Cu deficiency; CuSO<sub>4</sub> 0  $\mu$ M and 2  $\mu$ M caused mild Cu deficiency; CuSO<sub>4</sub> 5  $\mu$ M can be considered a Cu sufficiency growth

**Table 3**  
Identification of *cis*-elements in the promoter region of *SICOPTs*.

	COPT1	COPT2	COPT3	COPT4	COPT5	COPT6
<b>Micronutrient</b>						
Copper	2	16	4	8	16	16
Iron	1	0	0	0	0	0
<b>Macronutrient</b>						
Potassium	6	5	3	5	8	5
Sulfur	3	2	2	0	2	2
Phosphate	0	0	0	0	2	0
<b>Organ/tissue-specific</b>						
Seed	55	57	43	37	40	43
Endosperm	21	21	20	27	35	18
Embryo	3	4	2	6	10	3
Mesophyll	22	26	26	32	33	30
Root	30	22	22	28	26	22
Pollen	19	12	13	14	24	19
Fruit	0	1	0	0	2	0
<b>Hormones</b>						
ABA	20	19	19	26	19	10
Cytokinin	9	15	23	19	29	2
Gibberelin	8	13	4	8	11	7
SA	5	4	5	0	6	7
Auxin	6	4	3	3	6	2
Ethylene	4	2	0	2	0	4
JA	0	1	0	1	2	0
<b>Abiotic stress</b>						
Light	53	56	43	55	60	41
Water stress	12	19	9	18	19	6
Wounding	5	5	4	0	7	6
Temperature	1	4	3	1	10	6
CO <sub>2</sub>	0	2	4	0	3	2
Osmolarity	0	1	4	2	0	0
Anerobiosis	0	2	2	2	0	0
<b>Biotic stress</b>						
Pathogen response	18	14	14	11	25	11
Disease resistance	4	4	4	3	7	2
Defense response	3	1	0	0	0	1
<b>Others</b>						
Nodulation	6	8	6	12	10	10
Circadian clock	1	1	1	0	1	0

condition; CuSO<sub>4</sub> 10 μM possibly corresponds to mild Cu excess; CuSO<sub>4</sub> 100 μM imposes a severe Cu toxic environment for plant growth and development.

Leaves, stems and roots were cut from those seedlings and the *SICOPTs* transcript levels were separately analyzed in each tissue and condition (Fig. 6). In leaves, *SICOPT1*, *SICOPT2* and *SICOPT5* expressions continuously decreased with increasing Cu availability in growing media. The gene expression of *SICOPT3* and *SICOPT6*, however, peaked under both severe Cu deficiency and excess, and showed a minimum under Cu sufficiency condition. In contrast, the gene expression of *SICOPT2*, *SICOPT3*, *SICOPT5* and *SICOPT6* in stem bottomed down under mild Cu deficiency conditions. In turn, the *SICOPT1* transcript levels increased with Cu availability in this tissue. In roots, the transcript levels of all the *SICOPTs* were the highest for severe Cu deficiency. The gene expression of *SICOPT2*, *SICOPT3* and *SICOPT6* continuously lowered with increasing Cu availability. *SICOPT1* and *SICOPT5* bottomed down upon Cu sufficiency in this tissue. Cu excess increased *SICOPT1* and *SICOPT5*, but the gene expression levels were still lower than under severe Cu deficiency conditions (Fig. 6). The expression levels of *SICOPT4* were not detected under these experimental conditions.

#### 4. Discussion

Cu plays a dual role in plant growth and development as an essential

micronutrient and toxic highly-reactive element. To deal with this double-edge sword, plants display a complex regulatory network for Cu homeostasis by which a dynamic regulation of high-affinity Cu transporters (COPTs) is responsible for both the main Cu entrance from soil and its distribution throughout plant organs. Although COPTs have been identified in many different species [27,28,34–36,51,60–62], this gene family has not been characterized in *S. lycopersicum* even though tomato is the most consumed fruit worldwide and Cu deficiency detrimentally affects this crop's plant performance and yields [37–40].

In this study, six *SICOPT* genes were identified in the tomato genome, which extends the previous number of members mentioned for this family [27]. A conserved architecture based on three TMD and β-strains (Fig. 3) is shared between *SICOPTs* and their orthologs in other plant species, including monocots and dicots [27]. Nevertheless, in the phylogenetic analysis, *SICOPTs* clustered far from those of the monocots species, and were closer to vine VvCOPTs than to Arabidopsis members (dicots), which reflects a closer evolutionary relation of tomato to vine than to Arabidopsis or cereals (Fig. 1D and Fig. S2). The presence of different motifs required for these proteins to function is variable among *SICOPTs*' sequences. First, the Mx<sub>3</sub>Mx<sub>12</sub>Gx<sub>3</sub>G signature, which is essential for Cu sequestration and transmembrane translocation [63], was present in all the *SICOPTs*, except *SICOPT4*. Accordingly, *SICOPT4* clustered together with AtCOPT4, which has been reported to be incapable of Cu transport in the yeast *ctr1Δctr3Δ* mutant impaired for Cu uptake [61,63]. In addition, the M residue located 20 amino acids before TMD1 and the CxC motif located in the C-terminal region, which have been described as essential for Cu transport, and are related to Cu delivery and sensing in the cytoplasm, respectively [30,64], were not found in *SICOPT4*. The CxC motif was found in neither *SICOPT3* nor *SICOPT6*, which could mean that these members might be somehow impaired by Cu transfer to the metallochaperones inside the cell (Figs. 1 and 2).

In order to correlate these topology predictions with the functionality of the different *SICOPTs*, their experimental ability to rescue the defective growth of the *S. cerevisiae ctr1Δctr3Δ* mutant in respiratory and Fe-depleted medium was tested (Fig. 3). Thus, *SICOPT1* and *SICOPT2* appear to function alone and can replace the roles of ScCtr1 and ScCtr3 with Cu uptake in yeast (Fig. 3). In contrast, the deficient *ctr1Δctr3Δ* mutant growth on selective medium was rescued only partially by the expression of *SICOPT3* and *SICOPT5*, while no functional complementation was observed at all when expressing *SICOPT6* (Fig. 3). This might be interpreted as a lower affinity for Cu of *SICOPT3* and *SICOPT5*, as previously proposed for COPT members in other species [30,35,60,61]. It cannot be ruled out that these transporters and *SICOPT6* might need to form heterocomplexes to efficiently translocate Cu from the extracellular matrix to the cytosol, which is the case of most COPTs in *O. sativa* [28,65]. It should also be considered that *SICOPT3* and *SICOPT5* might locate to intracellular organelles rather than to the plasma membrane, which would partially explain their reduced complementation in the *ctr1Δctr3Δ* mutant. In Arabidopsis, AtCOPT3 and AtCOPT5 partially rescue the growth defects of a *ctr1Δctr3Δ* yeast mutant, locate in intracellular organelles, and are not regulated by SPL7 despite the presence of GTAC motifs (core of the Cu responsive elements) in their promoters [22,30,58,61]. *SICOPT3* and *SICOPT5* clustered close to these Arabidopsis proteins (Fig. 1D), but were predicted to be located in the plasma membrane with a 0.66 and 0.94 probability, respectively (Table 2). Despite the interaction network analyses indicating *SICOPT3* and *SICOPT5* as the two only *SICOPTs* to not interact with SPL7 (Fig. 2 and Fig. S3), both were significantly induced by severe Cu deficiency (Fig. 6). Therefore, further research is necessary to clarify the subcellular location of these proteins, and to understand their role in intracellular Cu recycling or extracellular Cu uptake in tomato.

The study of the *cis*-elements in the promoters of *SICOPTs* highlighted their putative regulation by hormones and abiotic stresses, especially ABA and light and water stresses, and with the nodulation process, the response to pathogens and the circadian clock (Table 3),

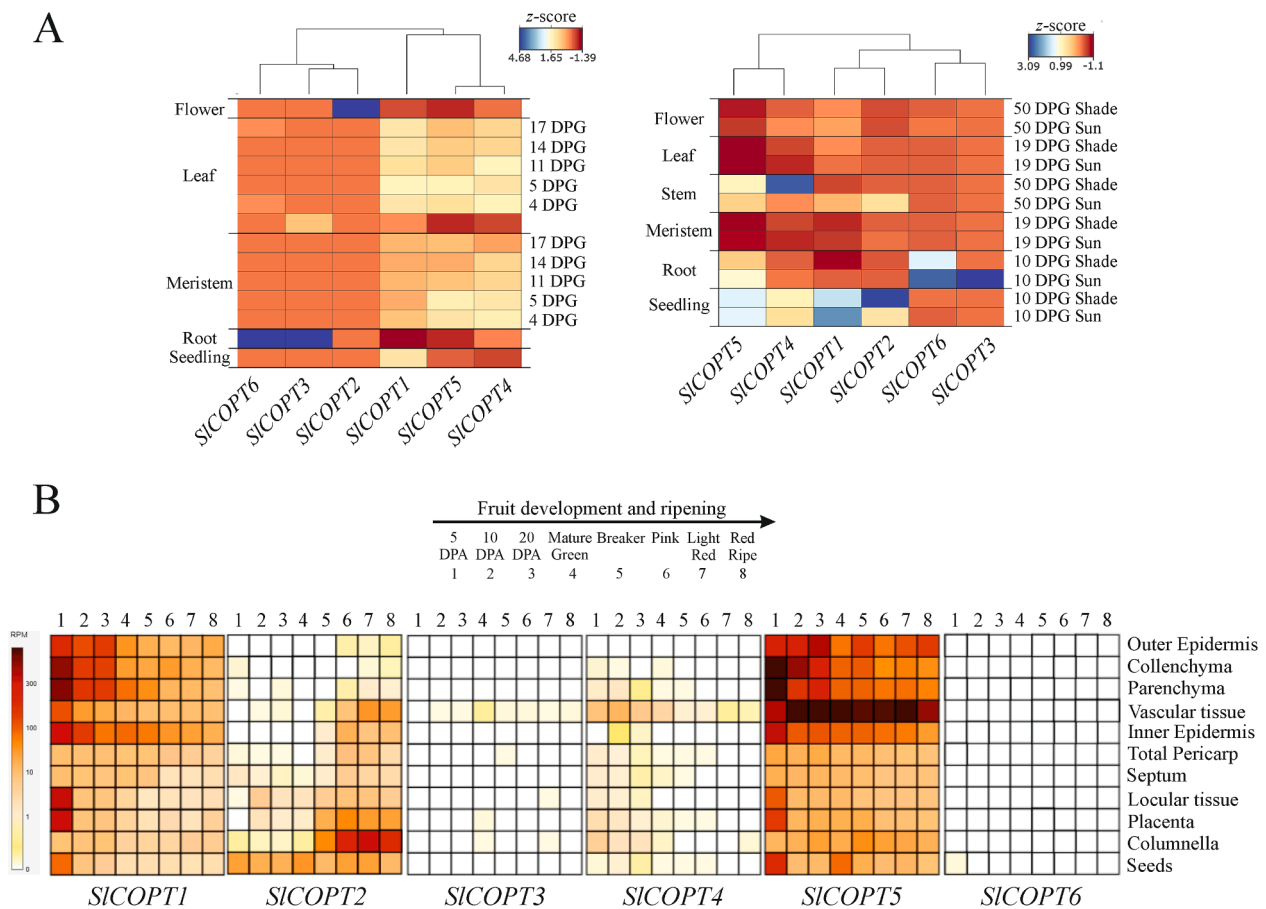


**Fig. 4.** *In silico* gene expression analyses. (A) Heatmap representation and hierarchical clustering of the *SICOPTs* gene expression in various tomato organs during development and in response to light stimuli. The transcriptional data from the TomExpress database were z-score-transformed. The bar indicates the colour scale applied for each experiment. DPG: days post-germination. (B) Heatmap of the tissue-specific *SICOPTs* expression during tomato fruit development and ripening, adapted from the Tomato Expression Atlas database. The bar denotes the colour scale for the RPM values. The numbers on heatmaps correspond to developmental and ripening stages, as indicated in the figure. DPA: days post-anthesis.

which agree with previous reports in different species [22,34,62,66]. This evidences a coordinated environmental and hormonal signaling for the purpose of optimizing Cu absorption and prioritizing it among other micronutrients by allowing essential functions and a dynamic response to surrounding fluctuations. The regulation of *SICOPTs* in response to Cu availability adds complexity to Cu homeostasis maintenance in tomato. Thus, GTAC motifs were found in all the *SICOPTs* (Table 3) and the expression levels of *SICOPTs* were mostly induced by low Cu levels (Fig. 6). A general expression pattern consisting of a concomitant lowering in transcript levels with increased Cu availability was found for *SICOPT1*, *SICOPT2* and *SICOPT5* in leaves and for *SICOPT2*, *SICOPT3* and *SICOPT6* in roots. Interestingly in stem tissue, the *SICOPT2*, *SICOPT3*, *SICOPT5* and *SICOPT6* transcript levels increased in response to not only Cu severe deficiency, but also to Cu excess, which occurred for *SICOPT3* and *SICOPT6* in leaf and for *SICOPT1* and *SICOPT5* in root tissues (Fig. 6). This demonstrates that the regulation of *SICOPTs* in response to suboptimal Cu levels, and probably tolerance to Cu stress, is organ-dependent. This pattern might be interpreted as a strategy to specifically translocate Cu inside the cell from the stem vasculature (or the leaf and root tissues to a lesser extent) under Cu toxic conditions to store Cu excess in the vacuole and to avoid tissue damage propagation. This idea is supported by the specialized expression of both *SICOPT5* in fruit vasculature and *SICOPT2* in the columnella (Fig. 4B). In line with this, similar expression patterns and organ-/tissue-specificities between two COPTs or more has been associated with a cooperative role in Cu transport [28,65]. In the present work, *SICOPT4* and *SICOPT5* showed similar vasculature-specialized expression patterns during fruit

development and ripening, and clustered together when the gene expression levels in different plant organs during development or in response to light were considered (Fig. 4). Similarly, *SICOPT3* and *SICOPT6* clustered together under these conditions, and both were barely expressed in fruit tissue (Fig. 4). These two members also responded similarly to Cu availability (Fig. 6). Last, *SICOPT1* and *SICOPT2* were inversely regulated during fruit development and ripening, and clustered on the same branch when gene expression levels in response to light stimuli were studied (Fig. 4). Therefore, it can be hypothesized that *SICOPT4* (even though its inability to transport Cu) and *SICOPT5*, and *SICOPT3* and *SICOPT6*, somehow cooperate to transport Cu in different tissues and developmental stages, which would explain the obtained functional assay results (Fig. 3). Furthermore, *SICOPT1* and *SICOPT2* appeared to be related in some extent and showed a coordinated response to different developmental or stress conditions, although the formation of heterocomplexes between them was not needed for their individual functionality.

The interaction network analyses revealed that *SICOPTs* were associated with a number of proteins related to Cu homeostasis (Fig. 2 and Fig. S3). Of them,  $P_{1B}$ -type ATPases (HMAs) are involved in Cu transport from the cytosol to different intracellular compartments through the hydrolysis of ATP [30], while COX11, CCS, ATOX1 and CCH are metallochaperones that deliver Cu to HMAs or Cu-demanding proteins [17]. *SICOPTs* are also related to other metal transporters, including those that are specific for Mg (MRS2s), Fe (OPT) and Zn (ZRT/IRT), and other more promiscuous transporting divalent metals (ZIPs) (Fig. 2 and Fig. S3), which agrees with both the different response of Cu absorption



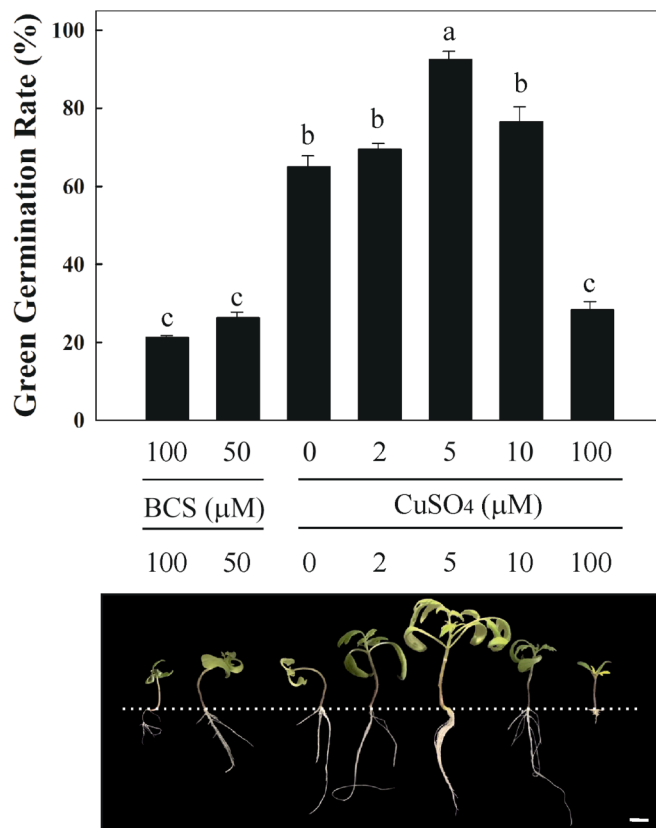


**Fig. 5.** Cu availability effects on tomato plant growth. The green germination rate calculated as the percentage of germinated tomato seeds developing true leaves when grown under different Cu availability conditions. Data represent the mean value of three biological replicates ± standard error. Representative images of the germinated 21-day-old seedlings are shown. A discontinuous line indicates the transition from root to stem to visualize differential growth. Scale bar: 1 cm.

in the presence of other metals and the interrelationship described for these elements [11,27,58,67].

Last, all the SICOPTs save SICOPT5 were associated with an interaction module composed of a protein phosphatase (PP2C), two protein kinases (YAK1 and DYRK3), a G protein subunit (GNB1) and three peroxins (PEX5, PEX7 and PEX10). Peroxisomes are essential for lipid metabolism, free radical detoxification and embryo development [68]. Indeed inside peroxisomes, Cu/Zn SODs detoxify the ROS generated during β-oxidation and other processes, which implies that Cu is required in this intracellular compartment. Reversible phosphorylation is a control mechanism for proteins in peroxisomes. It should be noted that PP2Cs require Mg and Mn as cofactors, and Zn is essential for PEX assembly and function [69–71]. Therefore, putative COPT-PEX-PP2C crosstalk makes sense in a scenario in which coordinated intracellular Cu distribution contributes to avoid throughout Cu/Zn SODs the ROS damage that might be caused by peroxisome activity.

### 5. Conclusion

This work bridges the knowledge gap about Cu uptake and transport in *S. lycopersicum*. Six putative SICOPT family members were identified and characterized by a range of *in silico* analyses. The conserved folding architecture of these proteins compared to COPTs in other species, together with their putative connections with other Cu homeostasis-related proteins, suggests that all SICOPTs but SICOPT4 are Cu transporters. Based on the ability of different SICOPTs to restore the growth of the *ctr1Δctr3Δ* yeast mutant on selective media, and the expression patterns of these genes in response to developmental and stressful cues

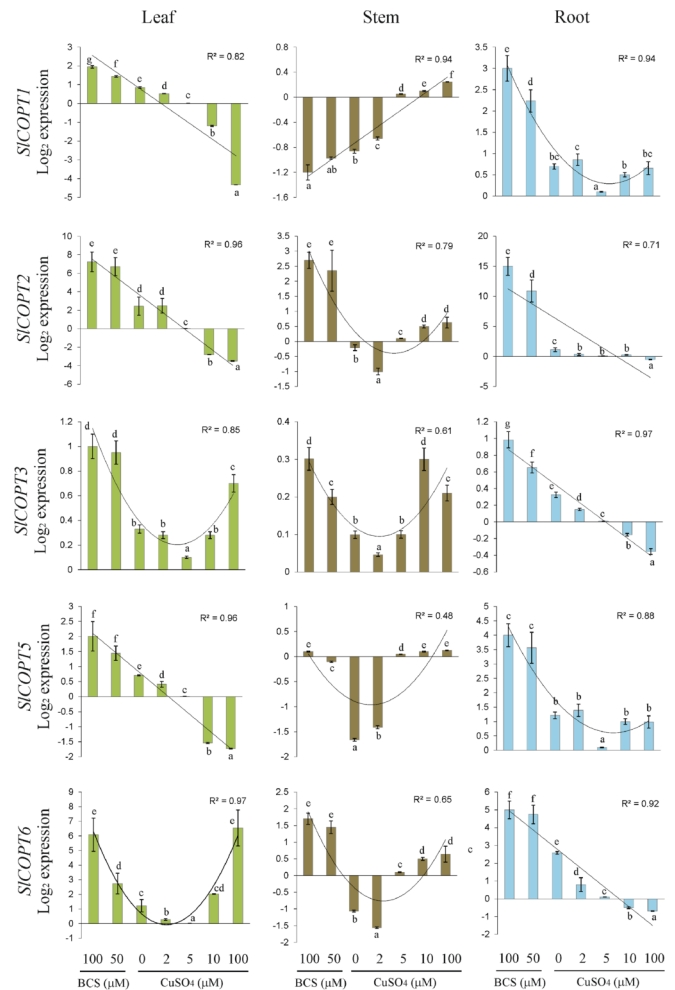


**Fig. 6.** Effect of Cu availability growing conditions on SICOPTs gene expression. The regression curve and the regression coefficient ( $R^2$ ) for each gene and tissue are included in every panel. Bars represent the mean values of three biological replicates ± standard error. Expression levels were relative to those obtained under the Cu sufficiency condition (CuSO<sub>4</sub> 5 μM) for each gene and tissue.

and to a range of Cu availability conditions, we argue that SICOPT1 and SICOPT2, which probably locate in the plasma membrane, are the only SICOPTs enabled to mediate Cu transport themselves, while SICOPT3 and SICOPT5 might be located in intracellular organelles and/or need other COPTs, such as SICOPT6 and SICOPT4, respectively, to perform that function. This work sets the basis for future research to develop biotechnological tools to help to improve tomato resilience under limiting Cu conditions and Cu phytoremediation of polluted soils.

### CRedit authorship contribution statement

**Paco Romero:** Conceptualization, Methodology, Formal analysis, Investigation, Writing – original draft, Writing – review & editing, Visualization, Supervision, Project administration, Funding acquisition. **Alessandro Gabrielli:** Formal analysis, Investigation, Writing – original draft. **Raúl Sampedro:** Methodology, Formal analysis, Investigation. **Ana Perea-García:** Methodology, Formal analysis, Investigation. **Sergi Puig:** Conceptualization, Writing – review & editing. **Maria Teresa Lafuente:** Conceptualization, Funding acquisition, Writing – review & editing.

## Declaration of competing interest

The authors declare that they have no known competing financial interests or personal relationships that could have appeared to influence the work reported in this paper.

## Acknowledgments

We thank Dr. L. Peñarubia (UV, Valencia, Spain) for providing the p426GPDATCOPT1 plasmid, for allowing us to use the required infrastructures for the *in vitro* assays, and for her helpful discussions. The technical assistance of J. Coll at the Microscopy Facility at the IATA-CSIC (Valencia, Spain) is also gratefully acknowledged. This work was supported by the TOMACOP Project as part of the Marie Skłodowska-Curie Actions and the European Horizon 2020 Programme (H2020-MSCA-IF-799712). We acknowledge support of the publication fee by the CSIC Open Access Publication Support Initiative through its Unit of Information Resources for Research (URICI).

## Appendix A. Supplementary data

Supplementary data to this article can be found online at <https://doi.org/10.1016/j.ijbiomac.2021.10.032>.

## References

- [1] B.J. Alloway, *Copper in Plant, Animal and Human Nutrition*, 1988.
- [2] M. DiDonato, B. Sarkar, Copper transport and its alterations in Menkes and Wilson diseases, *Biochim. Biophys. Acta - Mol. Basis Dis.* 1360 (1997) 3–16, [https://doi.org/10.1016/S0925-4439\(96\)00064-6](https://doi.org/10.1016/S0925-4439(96)00064-6).
- [3] R.G. Barber, Z.A. Grenier, J.L. Burkhead, Copper toxicity is not just oxidative damage: zinc systems and insight from Wilson disease, *Biomedicines* 9 (2021) 316, <https://doi.org/10.3390/biomedicines9030316>.
- [4] K. Socha, K. Klimiuk, S.K. Naliwajko, J. Soroczynska, A. Puscion-jakubik, R. Markiewicz-zukowska, J. Kochanowicz, Dietary habits, selenium, copper, zinc and total antioxidant status in serum in relation to cognitive functions of patients with alzheimer's disease, *Nutrients* 13 (2021) 1–14, <https://doi.org/10.3390/nu13020287>.
- [5] M. Bost, S. Houdart, M. Oberli, E. Kalonji, J.F. Huneau, I. Margaritis, Dietary copper and human health: current evidence and unresolved issues, *J. Trace Elem. Med. Biol.* 35 (2016) 107–115, <https://doi.org/10.1016/j.jtemb.2016.02.006>.
- [6] J.R. Prohaska, Long-term functional consequences of malnutrition during brain development: Copper, in: *Nutrition*, Elsevier, 2000, pp. 502–504, [https://doi.org/10.1016/S0899-9007\(00\)00308-7](https://doi.org/10.1016/S0899-9007(00)00308-7).
- [7] P. Marschner, Elsevier, 2012, <https://doi.org/10.1016/C2009-0-63043-9>.
- [8] M. Rehman, L. Liu, Q. Wang, M.H. Saleem, S. Bashir, S. Ullah, D. Peng, Copper environmental toxicology, recent advances, and future outlook: a review, *Environ. Sci. Pollut. Res.* 26 (2019) 18003–18016, <https://doi.org/10.1007/s11356-019-05073-6>.
- [9] I. Yruela, Copper in plants: acquisition, transport and interactions, *Funct. Plant Biol.* 36 (2009) 409–430, <https://doi.org/10.1071/FP08288>.
- [10] J.L. Burkhead, K.A. Gogolin Reynolds, S.E. Abdel-Ghany, C.M. Cohu, M. Pilon, Copper homeostasis, *New Phytol.* 182 (2009) 799–816, <https://doi.org/10.1111/j.1469-8137.2009.02846.x>.
- [11] A. Perea-García, A. García-Molina, N. Andrés-Colás, F. Vera-Sirera, M.A. Pérez-Amador, S. Puig, L. Peñarubia, Arabidopsis copper transport protein COPT2 participates in the cross talk between iron deficiency responses and low-phosphate signaling, *Plant Physiol.* 162 (2013) 180–194, <https://doi.org/10.1104/pp.112.212407>.
- [12] N. Andrés-Colás, A. Perea-García, S. Puig, L. Peñarubia, Deregulated copper transport affects Arabidopsis development especially in the absence of environmental cycles, *Plant Physiol.* 153 (2010) 170–184, <https://doi.org/10.1104/pp.110.153676>.
- [13] M. Rahmati Ishka, O.K. Vatamaniuk, Copper deficiency alters shoot architecture and reduces fertility of both gynoecium and androecium in Arabidopsis thaliana, *Plant, Direct* 4 (2020), e00288, <https://doi.org/10.1002/pld3.288>.
- [14] J. Yan, J.-C. Chia, H. Sheng, H. Jung, T.-O. Zavadna, L. Zhang, R. Huang, C. Jiao, E. J. Craft, Z. Fei, L.V. Kochian, O.K. Vatamaniuk, Arabidopsis pollen fertility requires the transcription factors CITF1 and SPL7 that regulate copper delivery to anthers and jasmonic acid synthesis, *Plant Cell* 29 (2017) 3012–3029, <https://doi.org/10.1105/tpc.17.00363>.
- [15] H. Sheng, Y. Jiang, M.R. Ishka, J.-C. Chia, T. Dokuchayeva, Y. Kavulych, T.-O. Zavadna, P. Mendoza, R. Huang, L. Smieshka, A. Woll, O. Terek, N. Romanyuk, Y. Zhou, O. Vatamaniuk, YSL3-mediated copper distribution is required for fertility, grain yield, and size in Brachypodium, *BioRxiv*. (2019), <https://doi.org/10.1101/2019.12.12.874396>.
- [16] V. Sancenón, S. Puig, I. Mateu-Andrés, E. Dorcey, D.J. Thiele, L. Peñarubia, The Arabidopsis copper transporter COPT1 functions in root elongation and pollen development, *J. Biol. Chem.* 279 (2004) 15348–15355, <https://doi.org/10.1074/jbc.M313321200>.
- [17] M. Migocka, K. Malas, Plant responses to copper: molecular and regulatory mechanisms of copper uptake, distribution and accumulation in plants, in: T. Kamiya, D.J. Burritt, L.-S.P. Tran, T. Fujiwara (Eds.), *Plant Micronutr. Use Effic. Mol. Genomic Perspect. Crop Plants*, Academic Press, 2018, pp. 71–86, <https://doi.org/10.1016/B978-0-12-812104-7.00005-8>.
- [18] U. Krämer, S. Clemens, Functions and homeostasis of zinc, copper, and nickel in plants, *Top. Curr. Genet.* 14 (2006) 216–271, [https://doi.org/10.1007/4735\\_96](https://doi.org/10.1007/4735_96).
- [19] A. Schulten, U. Krämer, in: *Interactions Between Copper Homeostasis and Metabolism in Plants*, Springer, Berlin Heidelberg, 2017, pp. 111–146, [https://doi.org/10.1007/124\\_2017\\_7](https://doi.org/10.1007/124_2017_7).
- [20] S. Puig, N. Andrés-Colás, A. García-Molina, L. Peñarubia, Copper and iron homeostasis in Arabidopsis: responses to metal deficiencies, interactions and biotechnological applications, *Plant Cell Environ.* 30 (2007) 271–290, <https://doi.org/10.1111/j.1365-3040.2007.01642.x>.
- [21] B.M. Waters, H.H. Chu, R.J. DiDonato, L.A. Roberts, R.B. Eisleys, B. Lahner, D. E. Salt, E.L. Walker, Mutations in arabidopsis yellow stripe-Like1 and yellow stripe-Like3 reveal their roles in metal ion homeostasis and loading of metal ions in seeds, *Plant Physiol.* 141 (2006) 1446–1458, <https://doi.org/10.1104/pp.106.082586>.
- [22] L. Peñarubia, P. Romero, A. Carrió-Seguí, A. Andrés-Bordería, J. Moreno, A. Sanz, Temporal aspects of copper homeostasis and its crosstalk with hormones, *Front. Plant Sci.* 6 (2015), <https://doi.org/10.3389/fpls.2015.00255>.
- [23] M. Bernal, D. Casero, V. Singh, G.T. Wilson, A. Grande, H. Yang, S.C. Dodani, M. Pellegrini, P. Huijser, E.L. Connolly, S.S. Merchant, U. Krämer, Transcriptome sequencing identifies SPL7-regulated copper acquisition genes FRO4/FRO5 and the copper dependence of iron homeostasis in Arabidopsis, *Plant Cell* 24 (2012) 738–761, <https://doi.org/10.1105/tpc.111.090431>.
- [24] K. Ravet, M. Pilon, Copper and iron homeostasis in plants: the challenges of oxidative stress, antioxidants redox, *Signal.* 19 (2013) 919–932, <https://doi.org/10.1089/ars.2012.5084>.
- [25] C.M. Cohu, M. Pilon, Cell biology of copper, *Plant Cell Monogr.* 17 (2010) 55–74, [https://doi.org/10.1007/978-3-642-10613-2\\_3](https://doi.org/10.1007/978-3-642-10613-2_3).
- [26] M. Pilon, Moving copper in plants, *New Phytol.* 192 (2011) 305–307, <https://doi.org/10.1111/j.1469-8137.2011.03869.x>.
- [27] R. Vatansever, I.I. Ozyigit, E. Filiz, Genome-wide identification and comparative analysis of copper transporter genes in plants, *Interdiscip. Sci. Comput. Life Sci.* 9 (2017) 278–291, <https://doi.org/10.1007/s12539-016-0150-2>.
- [28] M. Yuan, X. Li, J. Xiao, S. Wang, Molecular and functional analyses of COPT/Ctr-type copper transporter-like gene family in rice, *BMC Plant Biol.* 11 (2011) 69, <https://doi.org/10.1186/1471-2229-11-69>.
- [29] C.J. De Feo, S.G. Aller, V.M. Unger, A structural perspective on copper uptake in eukaryotes, in: *BioMetals*, Springer, 2007, pp. 705–716, <https://doi.org/10.1007/s10534-006-9054-7>.
- [30] L. Peñarubia, N. Andrés-Colás, J. Moreno, S. Puig, Regulation of copper transport in Arabidopsis thaliana: a biochemical oscillator? *J. Biol. Inorg. Chem.* 15 (2010) 29–36, <https://doi.org/10.1007/s00775-009-0591-8>.
- [31] X. Wu, D. Sinani, H. Kim, J. Lee, Copper transport activity of yeast Ctr1 is down-regulated via its C terminus in response to excess copper, *J. Biol. Chem.* 284 (2009) 4112–4122, <https://doi.org/10.1074/jbc.M807909200>.
- [32] H. Yamasaki, M. Hayashi, M. Fukazawa, Y. Kobayashi, T. Shikanai, SQUAMOSA promoter binding protein-like7 is a central regulator for copper homeostasis in Arabidopsis, *Plant Cell* 21 (2009) 347–361, <https://doi.org/10.1105/tpc.108.060137>.
- [33] S.R. Gayomba, H. Il Jung, J. Yan, J. Danku, M.A. Rutzke, M. Bernal, U. Krämer, L. V. Kochian, D.E. Salt, O.K. Vatamaniuk, The CTR/COPT-dependent copper uptake and SPL7-dependent copper deficiency responses are required for basal cadmium tolerance in a thaliana, *Metallomics* 5 (2013) 1262–1275, <https://doi.org/10.1039/c3mt00111c>.
- [34] Q. Wang, N. Wei, X. Jin, X. Min, Y. Ma, W. Liu, Molecular characterization of the COPT/Ctr-type copper transporter family under heavy metal stress in alfalfa, *Int. J. Biol. Macromol.* 181 (2021) 644–652, <https://doi.org/10.1016/j.ijbiomac.2021.03.173>.
- [35] H. Wang, H. Du, H. Li, Y. Huang, J. Ding, C. Liu, N. Wang, H. Lan, S. Zhang, Identification and functional characterization of the ZmCOPT copper transporter family in maize, *PLoS One.* 13 (2018), e0199081, <https://doi.org/10.1371/journal.pone.0199081>.
- [36] V. Martins, E. Bassil, M. Hanana, E. Blumwald, H. Gerós, Copper homeostasis in grapevine: functional characterization of the Vitis vinifera copper transporter 1, *Planta* 240 (2014) 91–101, <https://doi.org/10.1007/s00425-014-2067-5>.
- [37] P. Adams, C.J. Graves, G.W. Winsor, Effects of copper deficiency and liming on the yield, quality and copper status of tomatoes, lettuce and cucumbers grown in peat, *Sci. Hortic. (Amsterdam)* 9 (1978) 199–205, [https://doi.org/10.1016/0304-4238\(78\)90001-8](https://doi.org/10.1016/0304-4238(78)90001-8).
- [38] D.I. Arnon, P.R. Stout, The essentiality of certain elements in minute quantity for plants with special reference to copper, *Plant Physiol.* 14 (1939) 371–375, <https://doi.org/10.1104/pp.14.2.371>.
- [39] C.S. Piper, Investigations on copper deficiency in plants, *J. Agric. Sci.* 32 (1942) 143–178, <https://doi.org/10.1017/S0021859600047870>.
- [40] L.F. Bailey, J.S. McHargue, Copper deficiency in tomatoes, *Am. J. Bot.* 30 (1943) 558, <https://doi.org/10.2307/2437465>.
- [41] B. Hu, J. Jin, A.Y. Guo, H. Zhang, J. Luo, G. Gao, GSDS, 2.0: an upgraded gene feature visualization server, *Bioinformatics* 31 (2015) 1296–1297, <https://doi.org/10.1093/bioinformatics/btu817>.

- [42] D.T. Jones, Protein secondary structure prediction based on position-specific scoring matrices, *J. Mol. Biol.* 292 (1999) 195–202, <https://doi.org/10.1006/jmbi.1999.3091>.
- [43] K. Higo, Y. Ugawa, M. Iwamoto, T. Korenaga, Plant cis-acting regulatory DNA elements (PLACE) database: 1999, *Nucleic Acids Res.* 27 (1999) 297–300, <https://doi.org/10.1093/nar/27.1.297>.
- [44] F. Sievers, A. Wilm, D. Dineen, T.J. Gibson, K. Karplus, W. Li, R. Lopez, H. McWilliam, M. Remmert, J. Söding, J.D. Thompson, D.G. Higgins, Fast, scalable generation of high-quality protein multiple sequence alignments using clustal omega, *Mol. Syst. Biol.* 7 (2011) 539, <https://doi.org/10.1038/msb.2011.75>.
- [45] I. Letunic, P. Bork, Interactive tree of life (iTOL) v5: an online tool for phylogenetic tree display and annotation, *Nucleic Acids Res.* (2021), <https://doi.org/10.1093/nar/gkab301>.
- [46] G.E. Crooks, G. Hon, J.M. Chandonia, S.E. Brenner, WebLogo: a sequence logo generator, *Genome Res.* 14 (2004) 1188–1190, <https://doi.org/10.1101/gr.849004>.
- [47] J. Yang, R. Yan, A. Roy, D. Xu, J. Poisson, Y. Zhang, The I-TASSER suite: protein structure and function prediction, *Nat. Methods* 12 (2015) 7–8, <https://doi.org/10.1038/nmeth.3213>.
- [48] F. Ren, B.L. Logeman, X. Zhang, Y. Liu, D.J. Thiele, P. Yuan, X-ray structures of the high-affinity copper transporter Ctr1, *Nat. Commun.* 10 (2019) 1386, <https://doi.org/10.1038/s41467-019-09376-7>.
- [49] D. Szklarczyk, A.L. Gable, D. Lyon, A. Junge, S. Wyder, J. Huerta-Cepas, M. Simonovic, N.T. Doncheva, J.H. Morris, P. Bork, L.J. Jensen, C. Von Mering, STRING v11: protein-protein association networks with increased coverage, supporting functional discovery in genome-wide experimental datasets, *Nucleic Acids Res.* 47 (2019) D607–D613, <https://doi.org/10.1093/nar/gky1131>.
- [50] D. Mumberg, R. Müller, M. Funk, Yeast vectors for the controlled expression of heterologous proteins in different genetic backgrounds, *Gene* 156 (1995) 119–122, [https://doi.org/10.1016/0378-1119\(95\)00037-7](https://doi.org/10.1016/0378-1119(95)00037-7).
- [51] F.J. Escaray, C.J. Antonelli, G.J. Copello, S. Puig, L. Peñarrubia, O.A. Ruiz, A. Perea-García, Characterization of the copper transporters from *Lotus* spp. and their involvement under flooding conditions, *Int. J. Mol. Sci.* 20 (2019) 3136, <https://doi.org/10.3390/ijms20133136>.
- [52] M. Zouine, E. Maza, A. Djari, M. Lauvernier, P. Frasse, A. Smouni, J. Pirrello, M. Bouzayen, TomExpress, a unified tomato RNA-seq platform for visualization of expression data, clustering and correlation networks, *Plant J.* 92 (2017) 727–735, <https://doi.org/10.1111/tpj.13711>.
- [53] Y. Shinozaki, P. Nicolas, N. Fernandez-Pozo, Q. Ma, D.J. Evanich, Y. Shi, Y. Xu, Y. Zheng, S.I. Snyder, L.B.B.B. Martin, E. Ruiz-May, T.W. Thannhauser, K. Chen, D. S. Domozych, C. Catalá, Z. Fei, L.A. Mueller, J.J. Giovannoni, J.K.C.C. Rose, High-resolution spatiotemporal transcriptome mapping of tomato fruit development and ripening, *Nat. Commun.* 9 (2018) 364, <https://doi.org/10.1038/s41467-017-02782-9>.
- [54] N. Fernandez-Pozo, Y. Zheng, S.I. Snyder, P. Nicolas, Y. Shinozaki, Z. Fei, C. Catalá, J.J. Giovannoni, J.K.C. Rose, L.A. Mueller, The tomato expression atlas, *Bioinformatics* 33 (2017) 2397–2398, <https://doi.org/10.1093/bioinformatics/btx190>.
- [55] R.J. Pattison, F. Csukasi, Y. Zheng, Z. Fei, E. van der Knaap, C. Catalá, Comprehensive tissue-specific transcriptome analysis reveals distinct regulatory programs during early tomato fruit development, *Plant Physiol.* 168 (2015) 1684–1701, <https://doi.org/10.1104/pp.15.00287>.
- [56] T. Murashige, F. Skoog, A revised medium for rapid growth and bio assays with tobacco tissue cultures, *Physiol. Plant.* 15 (1962) 473–497, <https://doi.org/10.1111/j.1399-3054.1962.tb08052.x>.
- [57] P. Romero, J.K.C. Rose, A relationship between tomato fruit softening, cuticle properties and water availability, *Food Chem.* 295 (2019) 300–310, <https://doi.org/10.1016/j.foodchem.2019.05.118>.
- [58] A. Carrió-Seguí, P. Romero, C. Curie, S. Mari, L. Peñarrubia, Copper transporter COPT5 participates in the crosstalk between vacuolar copper and iron pools mobilisation, *Sci. Rep.* 9 (2019), <https://doi.org/10.1038/s41598-018-38005-4>.
- [59] P. Romero, F. Alférez, B. Establés-Ortiz, M.T. Lafuente, Insights into the regulation of molecular mechanisms involved in energy shortage in detached citrus fruit, *Sci. Rep.* 10 (2020) 1109, <https://doi.org/10.1038/s41598-019-57012-7>.
- [60] H.I. Jung, S.R. Gayomba, J. Yan, O.K. Vatamaniuk, *Brachypodium distachyon* as a model system for studies of copper transport in cereal crops, *Front. Plant Sci.* 5 (2014) 236, <https://doi.org/10.3389/fpls.2014.00236>.
- [61] V. Sancenón, S. Puig, H. Mira, D.J. Thiele, L. Peñarrubia, Identification of a copper transporter family in *Arabidopsis thaliana*, *Plant Mol. Biol.* 51 (2003) 577–587, <https://doi.org/10.1023/A:1022345507112>.
- [62] M. Senovilla, I. Abreu, V. Escudero, C. Cano, A. Bago, J. Imperial, M. González-Guerrero, MtCOPT2 is a Cu<sup>+</sup> transporter specifically expressed in *Medicago truncatula* mycorrhizal roots, *Mycorrhiza* (2020), <https://doi.org/10.1007/s00572-020-00987-3>.
- [63] S. Puig, Function and regulation of the plant COPT family of high-affinity copper transport proteins, *Adv. Bot.* 2014 (2014) 1–9, <https://doi.org/10.1155/2014/476917>.
- [64] Z. Xiao, A.G. Wedd, A C-terminal domain of the membrane copper pump Ctr1 exchanges copper(I) with the copper chaperone Atx1, *Chem. Commun.* 2 (2002) 588–589, <https://doi.org/10.1039/b111180a>.
- [65] M. Yuan, S. Wang, Z. Chu, X. Li, C. Xu, The bacterial pathogen *Xanthomonas oryzae* overcomes rice defenses by regulating host copper redistribution, *Plant Cell* 22 (2010) 3164–3176, <https://doi.org/10.1105/tpc.110.078022>.
- [66] A. Carrió-Seguí, P. Romero, A. Sanz, L. Peñarrubia, Interaction between ABA signaling and copper homeostasis in *Arabidopsis thaliana*, *Plant Cell Physiol.* 57 (2016) pcw087, <https://doi.org/10.1093/pcp/pcw087>.
- [67] Z. Zhai, S.R. Gayomba, H. Il Jung, N.K. Vimalakumari, M. Piñeros, E. Craft, M. A. Rutzke, J. Danku, B. Lahner, T. Punshon, M. Lou Guerinot, D.E. Salt, L. V. Kochian, O.K. Vatamaniuk, OPT3 is a phloem-specific iron transporter that is essential for systemic iron signaling and redistribution of iron and cadmium in *Arabidopsis*, *Plant Cell* 26 (2014) 2249–2264, <https://doi.org/10.1105/tpc.114.123737>.
- [68] L.L. Cross, H.T. Ebeed, A. Baker, Peroxisome biogenesis, protein targeting mechanisms and PEX gene functions in plants, *Biochim. Biophys. Acta - Mol. Cell Res.* 2016 (1863) 850–862, <https://doi.org/10.1016/j.bbamcr.2015.09.027>.
- [69] U. Schumann, J. Prestele, H. O'Geen, R. Brueggeman, G. Wanner, C. Gietl, Requirement of the C3HC4 zinc RING finger of the arabidopsis PEX10 for photorespiration and leaf peroxisome contact with chloroplasts, *Proc. Natl. Acad. Sci. U. S. A.* 104 (2007) 1069–1074, <https://doi.org/10.1073/pnas.0610402104>.
- [70] A.W. Woodward, B. Bartel, The *Arabidopsis* peroxisomal targeting signal type 2 receptor PEX7 is necessary for peroxisome function and dependent on PEX5, *Mol. Biol. Cell* 16 (2005) 573–583, <https://doi.org/10.1091/mbc.E04-05-0422>.
- [71] Y. Shi, Serine/threonine phosphatases: mechanism through structure, *Cell* 139 (2009) 468–484, <https://doi.org/10.1016/j.cell.2009.10.006>.